A Porous Media Approach for Analyzing a Countercurrent Dialyzer System

Yoshihiko Sano
Department of Mechanical Engineering,
Shizuoka University,
3-5-1 Johoku, Hamamatsu 432-8561, Japan

Akira Nakayama[1]
Department of Mechanical Engineering,
Shizuoka University,
3-5-1 Johoku, Hamamatsu 432-8561, Japan;
School of Civil Engineering
and Architecture,
Wuhan Polytechnic University,
Wuhan, Hubei 430023, China
e-mail: tmanaka@ipc.shizuoka.ac.jp

A porous media approach based on the volume-averaging theory has been proposed to investigate solute diffusion and ultrafiltration processes associated with hemodialysis using a hollow fiber membrane dialyzer. A general set of macroscopic governing equations has been derived for the three individual phases, namely, the blood phase, the dialysate phase, and the membrane phase. Thus, conservations of mass, momentum, and species are considered for blood compartments, dialysate compartments, and membranes within a dialyzer to establish a three concentration equation model. These macroscopic equations can be simultaneously solved for the various cases of inlet velocities of blood and dialysate. An analytic expression for the solute clearance was obtained for the one-dimensional case, in which important dimensionless parameters controlling the dialyzer system are identified for the first time. [DOI: 10.1115/1.4006104]

Keywords: dialyzer, mass transfer, ultrafiltration, porous media, volume averaging

Introduction

Hollow fiber dialyzers are widely used in the therapy of hemodialysis, which is a method for removing waste products such as creatinine and urea as well as free water from the blood when the kidneys are in renal failure. This dialyzer utilizes a bundle of hollow fibers of ultrafiltration membranes to remove metabolic end products from the human body. Mass diffusion and ultrafiltration processes through such membranes are most commonly described by Kedem–Katchalsky's model [1], which estimates the volume and solute flows of nonelectrolyte solutions across membranes. In this model, the total solute flux across the membranes is evaluated in consideration of the solutes diffusion rate through the membranes due to the difference of the concentration (i.e., transmembrane concentration) as well as the ultrafiltration flow induced by the transmembrane pressure and osmotic pressure.

A number of analytical and numerical models based on the Kedem–Katchalsky model have been reported in the literature. Lu and Lu [2] introduced a half channel model in which two parallel straight channels are considered for two fluids of different viscosities. They carried out numerical simulations for mass transfer through the porous membranes. Flat-plate membrane dialyzers were considered analytically by Tu et al. [3,4] for both concurrent and countercurrent dialysis systems. Their theoretical predictions agree qualitatively with their experimental results. Yeh [5] presented an analysis analogous to conventional heat exchanger analysis to consider the effect of external recycle on the performance of dialysis in double-pass rectangular membrane modules. Similar analyses were reported by Legallais et al. [6], Palaty et al. [7], Galach et al. [8], Yeh et al. [9], and Sigdell [10]. An excellent review on mathematical modeling of fluid and solute transport in hemodialysis may be found in Waniewski [11].

On the other hand, Ding et al. [12] accounted for both radial and axial gradients of the blood and dialysate sides, which were neglected in most of the previous investigations. In recent years, some numerical attempts have been made to simulate the fluid and solute transport processes in fiber membrane systems [13–15]. However, it appears to be impossible to resolve the details of flow and concentration within the dialyzer containing thousands of hollow fibers and dialysate compartments, even using a supercomputer available today, due to tremendous computational memory and CPU time required.

Under these situations, in which thousands of small-scale elements exist in a large space, the concept of local volume-averaging theory (VAT) is quite useful. This concept has been widely exploited in the study of porous media [16–20]. In VAT, one uses a grid system, which is just fine enough to resolve macroscopic flow and concentration fields. The idea is not to grid small-scale elements but to model them as a porous medium. A variety of models for the fiber membrane dialyzer have been proposed so far. Yet, the theory of porous media appears to be most appropriate for treating transport phenomena within hollow fiber dialyzers, since it contains fewer assumptions as compared to existing models.

In this study, two fluids in the dialyzer, namely, blood and dialysate, are considered in view of mass, momentum, and species conservation principles. Both blood and dialysate are treated as incompressible Newtonian fluids with constant properties. Blood exhibits non-Newtonian behavior only when the shear rates are very low. Within the dialyzers under usual operations, the shear rates are sufficiently large in all regions. Therefore, the bloods are assumed to be Newtonian everywhere as done by Shirazian et al. [13], Wang et al. [14], Kumar and Upadhyay [15], and many others. Furthermore, both blood and dialysate properties are assumed to be constant during the dialysis. This assumption is valid, since the concentrations of the waste products in the blood are sufficiently small.

A rigorous mathematical development based on the volume-averaging theory is presented to obtain a complete set of the three-dimensional volume-averaged governing equations for fiber membrane dialyzer systems. In this model, three individual concentrations are assigned for the blood, dialysate, and membranes. This three concentration equation model derived through the porous media approach for the first time can be used to account for the effect of countercurrent mass transfer between the blood phase and the dialysate phase through the membranes.

As a first step toward a complete three-dimensional numerical analysis, one-dimensional cases are considered to model typical dialyzer scenarios. Thus, the set of continuity, momentum, and concentration equations are simplified and eventually reduced to a set of analytic expressions for the concentrations and solute clearance. The important dimensionless groups, which control mass diffusion

[1]Corresponding author.

Contributed by the Heat Transfer Division of ASME for publication in the JOURNAL OF HEAT TRANSFER. Manuscript received August 19, 2011; final manuscript received November 21, 2011; published online May 24, 2012. Assoc. Editor: Andrey Kuznetsov.

and ultrafiltration processes associated with hemodialysis, are identified for the first time. The results are then compared against available experimental data to examine the validity of the present three-dimensional three concentration model.

Volume-Averaging Theory

In what follows, the porous media approach is introduced to derive a complete set of the volume-averaged governing equations for fiber membrane dialyzer systems. The procedure introduced by Nakayama and Kuwahara [20] for a general bioheat transfer model may readily be extended for the case of countercurrent dialysis system.

A local control volume V is considered in a fluid-saturated porous medium, as shown in Fig. 1, whose length scale $V^{1/3}$ is much smaller than the macroscopic characteristic length $V_c^{1/3}$, but, at the same time, much greater than the microscopic characteristic length (see e.g., Refs. [16,18]). Under this condition, the volume average of a certain variable ϕ is defined as

$$\langle \phi \rangle = \frac{1}{V}\int_{V_f} \phi dV \tag{1}$$

Another average, namely, intrinsic average, is given by

$$\langle \phi \rangle^f = \frac{1}{V_f}\int_{V_f} \phi dV \tag{2}$$

where V_f is the volume space which the fluid (blood or dialysate) occupies. Obviously, two averages are related as $\langle \phi \rangle = \varepsilon_f \langle \phi \rangle^f$, where $\varepsilon_f = V_f/V$ is the local volume fraction of the fluid space.

A variable may be decomposed into its intrinsic average and the spatial deviation from it

$$\phi = \langle \phi \rangle^f + \tilde{\phi} \tag{3}$$

This spatial decomposition is similar to the Reynolds decomposition used in the theory of turbulence, which separates the time average and fluctuating part. Naturally, its deviation $\tilde{\phi}$ is defined such that its spatial average equals zero. All dependent variables in the microscopic governing equations for the blood, dialysate, and membrane phases will be decomposed in this manner. One may utilize the following spatial average relationships:

$$\langle \phi_1 \phi_2 \rangle^f = \langle \phi_1 \rangle^f \langle \phi_2 \rangle^f + \left\langle \tilde{\phi}_1 \tilde{\phi}_2 \right\rangle^f \tag{4}$$

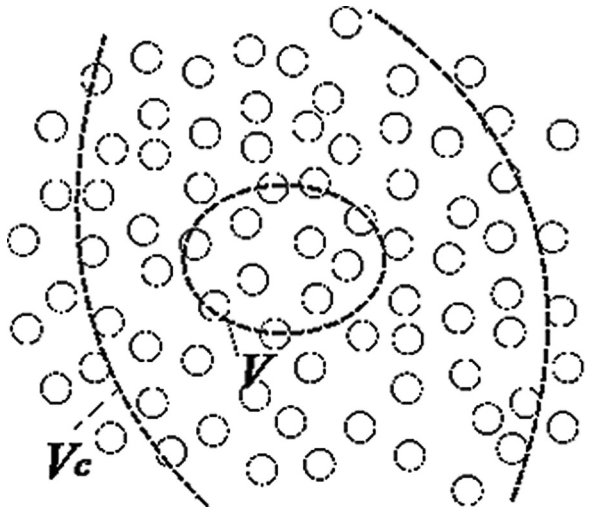

Fig. 1 Control volume in a porous medium

$$\left\langle \frac{\partial \phi}{\partial x_i} \right\rangle = \frac{\partial \langle \phi \rangle}{\partial x_i} + \frac{1}{V}\int_{A_{int}} \phi n_i dA \tag{5a}$$

$$\left\langle \frac{\partial \phi}{\partial x_i} \right\rangle^f = \frac{1}{\varepsilon_f}\frac{\partial \varepsilon_f \langle \phi \rangle^f}{\partial x_i} + \frac{1}{V_f}\int_{A_{int}} \phi n_i dA \tag{5b}$$

and

$$\left\langle \frac{\partial \phi}{\partial t} \right\rangle = \frac{\partial \langle \phi \rangle}{\partial t} \tag{6}$$

A_{int} represents the interfaces between the fluid and membrane matrix within the local control volume. Note n_i is the unit vector pointing outward from the fluid side to membrane matrix side.

Volume Fractions, Specific Areas, and Hydraulic Permeability of Dialyzer

Figure 2 depicts a hollow fiber membrane countercurrent dialyzer, in which only outer fibers are shown for clarity. In the porous media approach, one defines individual velocities and species concentrations to the three phases, namely, the blood, dialysate, and membrane phases. Each phase is treated as a continuum filling the entire space of the dialyzer case. Thus, three phases share the same space but with different volume fractions. Assigning the subscripts, b, d, and m to the blood phase, dialysate phase, and membrane phase, respectively, the following relations can be found for the volume fractions: ε_b, ε_m, and ε_d, the specific surface area of the blood compartment a_b (i.e., the total inner wall surface area of the hollow fibers per unit volume), and that of the dialysate compartment a_d (i.e., the total outer wall surface area of the hollow fibers per unit volume)

$$\varepsilon_b = \frac{N\frac{\pi}{4}d_b^2}{A} \tag{7a}$$

$$\varepsilon_m = \frac{\frac{\pi}{4}\left((d_b + 2t_m)^2 - d_b^2\right)}{\frac{\pi}{4}d_b^2}\varepsilon_b = 4\frac{t_m}{d_b}\left(1 + \frac{t_m}{d_b}\right)\varepsilon_b \tag{7b}$$

$$\varepsilon_d = 1 - \left(1 + 4\frac{t_m}{d_b}\left(1 + \frac{t_m}{d_b}\right)\right)\varepsilon_b \tag{7c}$$

$$a_b = \frac{4\varepsilon_b}{d_b} \tag{8a}$$

$$a_d = \frac{4\varepsilon_b}{d_b}\left(1 + 2\frac{t_m}{d_b}\right) \tag{8b}$$

Note that N is the number of hollow fibers, while A is the cross-sectional area of the dialyzer case. The membrane thickness, the

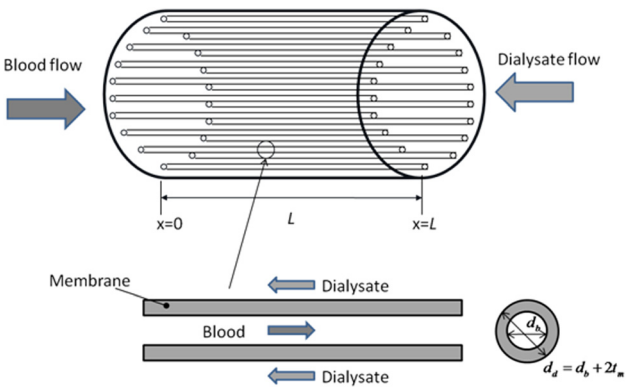

Fig. 2 Dialyzer system

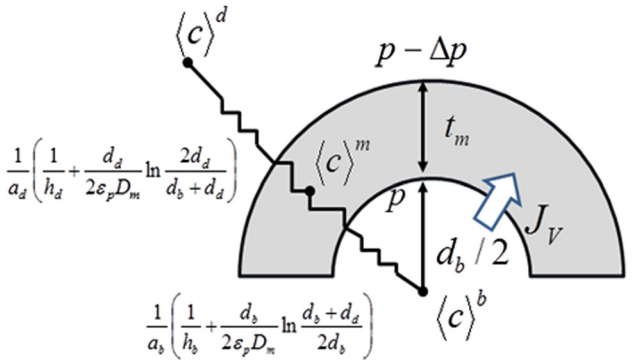

Fig. 3 Ultrafiltration through a membrane

inner, and outer diameters of the hollow fiber are indicated by t_m, d_b, and $d_d = d_b + 2t_m$, respectively.

Another important parameter in addition to the foregoing geometrical parameters is the permeability of the membranes, which controls the ultrafiltration velocity. Referring to Fig. 3, one may consider the radial Darcy flow through the membranes of the intrinsic permeability of the membrane K_m and find the relationship between the ultrafiltration velocity J_v and the transmembrane pressure Δp as follows:

$$J_V = L_p \Delta p \tag{9}$$

where

$$L_p = \frac{1}{\frac{\mu}{K_m}\frac{d_b}{2}\ln\left(1 + \frac{2t_m}{d_b}\right)} \tag{10}$$

is the hydraulic permeability of the porous membranes. This equation may be modified to account for the osmotic pressure Π

$$J_V = L_p(\Delta p - \Pi) \tag{11}$$

However, in a hemodialysis, it is a common practice to control the osmotic pressure between the blood and dialysate (around 3000 mOsm/l), such that $\Pi = 0$. The intrinsic permeability of the membranes with cylindrical pores of the diameter d_p and porosity ε_p may be evaluated from

$$K_m = \varepsilon_p d_p^2/32 \tag{12}$$

assuming on the Hagen–Poiseuille equation. In reality, the structure of the membranes is not available. Instead, the hydraulic permeability of the membrane L_p is provided.

Macroscopic Governing Equations

The microscopic governing equations, namely, the continuity, momentum, and species mass transfer equations can be written as follows:

$$\frac{\partial u_j}{\partial x_j} = 0 \tag{13}$$

$$\rho\frac{\partial u_i}{\partial t} + \rho\frac{\partial u_j u_i}{\partial x_j} = -\frac{\partial p}{\partial x_i} + \mu\frac{\partial^2 u_i}{\partial x_j^2} \tag{14}$$

$$\frac{\partial c}{\partial t} + \frac{\partial u_j c}{\partial x_j} = D\frac{\partial^2 c}{\partial x_j^2} \tag{15}$$

These governing equations may be written for the three individual phases and all dependent variables for the blood, dialysate, and membranes are decomposed according to Eq. (3). Then, these microscopic equations are integrated over the local control volume, exploiting the foregoing spatial average relationships. The set of the macroscopic governing equations thus obtained for the blood (lumen) flow may be given as follows:

$$\frac{\partial \varepsilon_b \langle u_j \rangle^b}{\partial x_j} + \int_{A_{int}} u_j n_{bj} dA = 0 \tag{16}$$

$$\rho\frac{\partial \langle u_i \rangle^b}{\partial t} + \rho\frac{\partial \langle u_j \rangle^b \langle u_i \rangle^b}{\partial x_j} = -\frac{\partial \langle p \rangle^b}{\partial x_i} + \frac{\partial}{\partial x_j}\left(\mu\frac{\partial \langle u_i \rangle^b}{\partial x_j} + \frac{\mu}{V_b}\int_{V_{b_{int}}} u_i dA - \rho\langle \tilde{u}_i \tilde{u}_j \rangle^b\right) + \frac{1}{V_b}\int_{A_{b_{int}}}\left(\mu\frac{\partial u_i}{\partial x_j} - p\delta_{ij}\right) n_{bj} dA - \frac{1}{V_b}\int_{A_{b_{int}}} \rho u_j u_i n_{bj} dA \tag{17}$$

$$\frac{\partial \varepsilon_b \langle c \rangle^b}{\partial t} + \frac{\partial \varepsilon_b \langle u_j \rangle^b \langle c \rangle^b}{\partial x_j} = \frac{\partial}{\partial x_j}\left(\varepsilon_b D_b \frac{\partial \langle c \rangle^b}{\partial x_j} + \frac{D_b}{V}\int_{A_{b_{int}}} c n_{b_j} dA - \rho\varepsilon_b \langle \tilde{c}\tilde{u}_j \rangle^b\right) + \frac{1}{V}\int_{A_{b_{int}}} D_b \frac{\partial c}{\partial x_j} n_{bj} dA - \frac{1}{V}\int_{A_{b_{int}}} c u_j n_{bj} dA \tag{18}$$

where the superscript b is assigned to indicate the blood phase intrinsic average quantities as defined by Eq. (2). Note that n_{bj} is the unit vector pointing outward from the blood side to membrane side.

Closure and Three Concentration Model for Dialyzer

These macroscopic equations may be modeled as follows:

$$\frac{\partial \varepsilon_b \langle u_j \rangle^b}{\partial x_j} + \omega = 0 \tag{19}$$

$$\rho\frac{\partial \langle u_i \rangle^b}{\partial t} + \rho\frac{\partial \langle u_j \rangle^b \langle u_i \rangle^b}{\partial x_j} = -\frac{\partial \langle p \rangle^b}{\partial x_i} + \mu\frac{\partial^2 \langle u_i \rangle^b}{\partial x_j^2} - \frac{\mu}{K_{b_{ij}}}\varepsilon_b \langle u_j \rangle^b \tag{20}$$

$$\frac{\partial \varepsilon_b \langle c \rangle^b}{\partial t} + \frac{\partial \varepsilon_b \langle u_j \rangle^b \langle c \rangle^b}{\partial x_j} = \frac{\partial}{\partial x_j}\left(\varepsilon_b D_b \frac{\partial \langle c \rangle^b}{\partial x_j} + \varepsilon_b D_{b\,dis_{jk}} \frac{\partial \langle c \rangle^b}{\partial x_k}\right) - a_b h_{tb}\left(\langle c \rangle^b - \langle c \rangle^m\right) - \omega \langle c \rangle^b \tag{21}$$

where $D_{b\,dis_{jk}}$ is the dispersion diffusivity tensor and

$$\omega = a_b J_v = \frac{1}{V}\int_{A_{b_{int}}} u_j n_{b_j} dA \tag{22}$$

is the perfusion rate (1/s), which is the product of the specific area a_b and ultrafiltration velocity J_v, describing the ultrafiltration volume rate of the blood per unit volume of the dialyzer, bleeding-off to the dialysate compartment through the membranes.

The concentration on the lumen (blood side) interface is assumed to be locally uniform such that its surface integral associate with the tortuosity

$$\frac{D_b}{V}\int_{A_{b_{int}}} c\ n_{b_j} dA$$

vanishes. Furthermore, the ultrafiltration velocity vector is assumed to be perpendicular to the lumen wall surface and uniform such that

$$\frac{\mu}{V_b}\int_{A_{b_{int}}} u_i dA = \frac{\mu}{V_b} J_v \int_{A_{b_{int}}} n_i dA = \vec{0}$$

vanishes. Likewise, the momentum bleed-off rate

$$\frac{1}{V}\int_{A_{b_{int}}} \rho u_j u_i n_{bj} dA \cong \rho\omega \frac{1}{A_{b_{int}}}\int_{A_{b_{int}}} u_i dA = \rho\omega J_v \int_{A_{b_{int}}} n_i dA = \vec{0}$$

also vanishes, since $u_i = J_v n_i$.

As for the macroscopic momentum equation, the Darcy expression is introduced for the flow resistance

$$\frac{1}{V_b}\int_{A_{b_{int}}} \left(\mu\frac{\partial u_i}{\partial x_j} - p\delta_{ij}\right) n_{bj} dA - \frac{\partial}{\partial x_j}\left(\rho\langle\tilde{u}_i\tilde{u}_j\rangle^b\right) = -\frac{\mu}{K_{b_{ij}}}\varepsilon_b\langle u_j\rangle^b \tag{23}$$

where the permeability tensor is given by

$$\frac{1}{K_{b_{ij}}} = \begin{bmatrix} \frac{1}{K_{bxx}} & 0 & 0 \\ 0 & \frac{1}{K_{byy}} & 0 \\ 0 & 0 & \frac{1}{K_{bzz}} \end{bmatrix} \tag{24}$$

$$K_{b_{xx}} = \frac{\varepsilon_b d_b^2}{32} \gg K_{b_{yy}} = K_{b_{zz}} \tag{25}$$

The axial permeability component $K_{b_{xx}}$ was estimated assuming laminar fully developed flow in a tube, while the transverse components $K_{b_{yy}} = K_{b_{zz}}$ may virtually be set to zero, since it is unlikely that the filtrated blood re-enters into the other hollow fibers. The axial dispersion diffusivity component may be given following Nakayama et al. [21] as:

$$D_{bdis_{xx}} = \frac{D_b}{192}\left(\frac{\langle u\rangle^b d_b}{D_b}\right)^2 \gg D_{bdis_{yy}} = D_{bdis_{zz}} \tag{26}$$

while the transverse components may be neglected as compared with the axial one. The solute bleed-off rate may be modeled as

$$\frac{1}{V}\int_{A_{b_{int}}} cu_j n_{bj} dA = \omega\langle c\rangle^b \tag{27}$$

For the interfacial mass transfer, the effective mass transfer coefficient may be introduced as

$$\frac{1}{V}\int_{A_{b_{int}}} D_b\frac{\partial c}{\partial x_j} n_{bj} dA = a_b h_{tb}\left(\langle c\rangle^b - \langle c\rangle^m\right) \tag{28}$$

where the effective mass transfer coefficient h_{tb} for the case of negligible tortuosity within the membrane is defined, referring to Fig. 3, as

$$\frac{1}{h_{tb}} = \frac{1}{h_b} + \frac{d_b}{2\varepsilon_p D_m}\ln\left(\frac{\frac{d_b + d_d}{2}}{d_b}\right) = \frac{1}{h_b} + \frac{d_b}{2\varepsilon_p D_m}\ln\left(1 + \frac{t_m}{d_b}\right) \tag{29}$$

where D_m is the solute diffusion coefficient in water.

Likewise, the set of the macroscopic equations for the dialysate (shell) flow may be written with subscript and superscript d as

$$\frac{\partial\varepsilon_d\langle u_j\rangle^d}{\partial x_j} - \omega = 0 \tag{30}$$

$$\rho\frac{\partial\langle u_i\rangle^d}{\partial t} + \rho\frac{\partial\langle u_j\rangle^d\langle u_i\rangle^d}{\partial x_j} = -\frac{\partial\langle p\rangle^d}{\partial x_i} + \mu\frac{\partial^2\langle u_i\rangle^d}{\partial x_j^2} - \frac{\mu}{K_{d_{ij}}}\varepsilon_d\langle u_j\rangle^d \tag{31}$$

$$\frac{\partial\varepsilon_d\langle c\rangle^d}{\partial t} + \frac{\partial\varepsilon_d\langle u_j\rangle^d\langle c\rangle^d}{\partial x_j} = \frac{\partial}{\partial x_j}\left(\varepsilon_d D_d\frac{\partial\langle c\rangle^d}{\partial x_j} + \varepsilon_d D_{d\,dis_{jk}}\frac{\partial\langle c\rangle^d}{\partial x_k}\right) - a_d h_{td}\left(\langle c\rangle^d - \langle c\rangle^m\right) + \omega\langle c\rangle^m \tag{32}$$

The axial permeability component may be evaluated using the hydraulic diameter concept as

$$K_{d_{xx}} = \frac{\varepsilon_d}{32}\left(\frac{4}{\pi d_d}\frac{\varepsilon_d\pi d_b^2}{\varepsilon_b 4}\right)^2 = \frac{\varepsilon_d}{32}\left(\frac{\varepsilon_d d_b^2}{\varepsilon_b d_d}\right)^2 \tag{33}$$

while the transverse components may be estimated according to Kuwahara et al. [22] as

$$K_{d_{yy}} = K_{d_{zz}} = \frac{\varepsilon_d^3 d_d^2}{120(1-\varepsilon_d)^2} \tag{34}$$

The axial dispersion diffusivity component may be estimated using the hydraulic concept as

$$D_{ddis_{xx}} = \frac{D_d}{192}\left(\frac{\langle u\rangle^d}{D_d}\left(\frac{\varepsilon_d {d_b}^2}{\varepsilon_b d_d}\right)\right)^2 \gg D_{ddis_{yy}} = D_{ddis_{zz}} \tag{35}$$

The transverse dispersion diffusivity components $D_{d\,dis_{yy}}$ and $D_{d\,dis_{zz}}$ are usually as small as 1/20 of the axial dispersion counterpart [23] and their effects may well be neglected.

Note that the mass transfer from the membranes to the dialysate compartment is estimated as

$$-\frac{1}{V}\int_{A_{d_{int}}} cu_j n_{dj} dA = \omega\langle c\rangle^m \tag{36}$$

while the interfacial mass transfer between the membrane to the dialysate is modeled as

$$\frac{1}{V}\int_{A_{d_{int}}} D_d\frac{\partial c}{\partial x_j} n_{d_j} dA = a_d h_{td}\left(\langle c\rangle^d - \langle c\rangle^m\right) \tag{37}$$

where

$$\frac{1}{h_{td}} = \frac{1}{h_d} + \frac{d_d}{2\varepsilon_p D_m}\ln\left(\frac{d_d}{\frac{d_b + d_d}{2}}\right) = \frac{1}{h_d} + \frac{d_b}{2\varepsilon_p D_m}\left(1 + 2\frac{t_m}{d_b}\right)\ln\left(\frac{1 + 2\frac{t_m}{d_b}}{1 + \frac{t_m}{d_b}}\right) \tag{38}$$

Although the ultrafiltration takes place radially outward from the lumen to shell compartments through the membranes, the macroscopic velocity resulting from such microscopically radial flow vanishes within the membrane continuum. Thus, as for the membrane phase, one only needs to consider the species concentration equation

$$\frac{\partial\varepsilon_m\langle c\rangle^m}{\partial t} = \frac{\partial}{\partial x_j}\left(\varepsilon_m D_{m_{jk}}\frac{\partial\langle c\rangle^m}{\partial x_k}\right) + a_b h_{tb}\left(\langle c\rangle^b - \langle c\rangle^m\right) + \omega\langle c\rangle^b + a_d h_{td}\left(\langle c\rangle^d - \langle c\rangle^m\right) - \omega\langle c\rangle^m \tag{39}$$

where $D_{mxx} \gg D_{myy} = D_{mzz}$ such that the transverse diffusion may be neglected as compared with the axial one. This completes the closure procedure. The present three concentration equation model consists of the continuity, momentum, and concentration equations for the blood and dialysate compartments, (19)–(21), (30)–(32), and the concentration equation for the membrane (39) along with the ultrafiltration velocity relationship, namely, Eqs. (9) and (22). This set of three concentration equations in the form of partial differential equations can be numerically integrated to reveal the details of the flow and concentration fields within a three-dimensional dialyzer, for the given initial and boundary conditions using any standard numerical procedure [18].

As a first step toward a complete three-dimensional numerical analysis, this study first considers a one-dimensional counterflow case which models typical dialyzer scenarios. The results are then compared against available experimental data to examine the validity of the present three-dimensional three concentration model. Although some previous work on counterflow in biosystems [24] is available, a counterflow with ultrafiltration has not been treated as completely as done in the present study.

One-Dimensional Three Concentration Model for Dialyzer

In what follows, the steady one-dimensional case is treated. An analytic solution is derived to examine the validity of the present three concentration model.

Velocity Fields. For this case, Eqs. (19)–(21), (30)–(32), and (39) are reduced to

$$\frac{du_b}{dx} = -\frac{du_d}{dx} = -\omega = -a_b J_v = -a_b L_p \left(\langle p \rangle^b - \langle p \rangle^d \right) \tag{40}$$

$$-\frac{d\langle p \rangle^b}{dx} - \frac{\mu}{K_{bxx}} u_b = 0 \tag{41}$$

$$-\frac{d\langle p \rangle^d}{dx} - \frac{\mu}{K_{dxx}} u_d = 0 \tag{42}$$

$$\frac{d}{dx} u_b \langle c \rangle^b = -a_b h_{tb} \left(\langle c \rangle^b - \langle c \rangle^m \right) - \omega \langle c \rangle^b \tag{43}$$

$$\frac{d}{dx} u_d \langle c \rangle^d = -a_d h_{td} \left(\langle c \rangle^d - \langle c \rangle^m \right) + \omega \langle c \rangle^m \tag{44}$$

$$a_b h_{tb} \left(\langle c \rangle^b - \langle c \rangle^m \right) + \omega \langle c \rangle^b + a_d h_{td} \left(\langle c \rangle^d - \langle c \rangle^m \right) - \omega \langle c \rangle^m = 0 \tag{45}$$

where the axial Darcian velocities of the blood and dialysate flows are denoted by

$$u_b = \varepsilon_b \langle u \rangle^b \tag{46a}$$

and

$$u_d = \varepsilon_d \langle u \rangle^d \tag{46b}$$

The boundary effects (i.e., Brinkman term) may be appreciable in small regions very close to the dialyzer case walls. There, the Darcian velocity shows its dependence on the transverse direction. However, the blood and dialysate flows within the fiber and dialysate compartments are most likely to be laminar and fully developed except small regions near the entrances. Thus, in this one-dimensional analysis, the inertia and Brinkman terms in the momentum equations are neglected. Furthermore, in all three concentration equations, the macroscopic diffusion terms are dropped, since such effects on the solute mass transfer would be negligibly small compared with those of the interfacial mass transfer and ultrafiltration. The continuity equation (40) gives

$$u_b + u_d = C_u = \text{const.} \tag{47}$$

Note that u_b is positive, while u_d is negative. Moreover, the dialysate inlet velocity is often higher than the blood inlet velocity, so that the constant C_u is likely to be negative. Subtracting Eq. (42) from Eq. (41), and then substituting Eq. (47), one obtains

$$-\frac{d}{dx}\left(\langle p \rangle^b - \langle p \rangle^d \right) = \mu \left(\frac{1}{K_{bxx}} + \frac{1}{K_{dxx}} \right) u_b - \frac{\mu}{K_{dxx}} C_u$$

Equation (40) may be used to eliminate the transmembrane pressure $(\langle p \rangle^b - \langle p \rangle^d)$ in the foregoing equation to obtain the second-order ordinary differential equation for u_b as follows:

$$\frac{d^2 u_b}{dx^2} = a_b L_p \mu \left(\frac{1}{K_{b_{xx}}} + \frac{1}{K_{d_{xx}}} \right) \left(u_b - \frac{C_u}{1+\alpha} \right) \tag{48}$$

which can readily be solved as

$$u_b(x*) = \frac{C_u}{1+\alpha} + \frac{\left(u_b(0) - \frac{C_u}{1+\alpha} \right) \sinh(B(1-x^*)) + \left(\frac{\alpha C_u}{1+\alpha} - u_d(1) \right) \sinh B x^*}{\sinh B} \tag{49}$$

where

$$\alpha = \frac{K_{d_{xx}}}{K_{b_{xx}}} \tag{50a}$$

is the permeability ratio (i.e., lumen and shell resistance ratio) and

$$B = L \sqrt{a_b L_p \mu \left(\frac{1}{K_{b_{xx}}} + \frac{1}{K_{d_{xx}}} \right)} = \frac{L}{d_b} \sqrt{8 \varepsilon_b \frac{K_m \left(\frac{1}{K_{b_{xx}}} + \frac{1}{K_{d_{xx}}} \right)}{\ln\left(1 + \frac{2t_m}{d_b} \right)}} \tag{50b}$$

is the dimensionless parameter associated with the membrane permeability. Moreover

$$x^* = \frac{x}{L} \tag{50c}$$

is the dimensionless coordinate, where L is the length of the dialyzer case, as indicated in Fig. 2. In Eq. (49), the inlet Darcian velocity of the blood $u_b(0)$ and that of the dialysate $u_d(1)$ are used, since they are the ones which are usually provided. The unknown constant C_u may be determined from the continuity relationship, namely, Eq. (40)

$$\omega(x^*) = -\frac{du_b}{dx} = a_b L_p \left(\langle p \rangle^b - \langle p \rangle^d \right) = \frac{B}{L} \frac{\left(u_b(0) - \frac{C_u}{1+\alpha} \right) \cosh(B(1-x^*)) - \left(\frac{\alpha C_u}{1+\alpha} - u_d(1) \right) \cosh B x^*}{\sinh B} \tag{51}$$

which can be solved for C_u for the given transmembrane pressure at $x = 0$ $\left(\langle p \rangle^b - \langle p \rangle^d \right)\Big|_{x*=0}$, as

$$C_u = \frac{1+\alpha}{\alpha + \cosh B} \left(u_b(0) \left(\cosh B - \frac{\sinh B}{B} \beta \right) + u_d(1) \right) \tag{52}$$

where

$$\beta = \frac{La_b L_p \left(\langle p\rangle^b - \langle p\rangle^d\right)\Big|_{x^*=0}}{u_b(0)} = \frac{8\varepsilon_b K_m L}{\mu u_b(0) d_b^2 \ln\left(1+\frac{2t_m}{d_b}\right)} \left(\langle p\rangle^b - \langle p\rangle^d\right)\Big|_{x^*=0} \tag{53}$$

is another important dimensionless parameter, namely, the dimensionless transmembrane pressure at the inlet.

Solute Concentration Fields. Having established the velocity field, Eq. (45) may readily be solved for the membrane concentration $\langle c\rangle^m$ as

$$\langle c\rangle^m = \frac{a_b h_{tb} + \omega}{a_b h_{tb} + a_d h_{td} + \omega}\langle c\rangle^b + \frac{a_d h_{td}}{a_b h_{tb} + a_d h_{td} + \omega}\langle c\rangle^d \tag{54}$$

which can be substituted into Eq. (44) as

$$\frac{d}{dx} u_d \langle c\rangle^d = \frac{a_d h_{td}(a_b h_{tb} + \omega)}{a_b h_{tb} + a_d h_{td} + \omega}\left(\langle c\rangle^b - \langle c\rangle^d\right) + \omega\langle c\rangle^m \tag{55}$$

It is interesting to note that the foregoing Eq. (55) along with Eq. (54) is quite similar to Kedem–Katchalsky model [1] as introduced by Waniewski et al. [25], Galach et al. [8], and many others. Kedem–Katchalsky model, for the case of negligible osmotic pressure and solute reflection coefficient, can be written as

$$\frac{d}{dx} u_d \langle c\rangle^d = a_b\left(P_m\left(\langle c\rangle^b - \langle c\rangle^d\right) + J_v\langle c\rangle^m\right) \tag{56}$$

and

$$\langle c\rangle^m = \left(1 - \frac{1}{\mathrm{Pe}} + \frac{1}{\exp(\mathrm{Pe}) - 1}\right)\langle c\rangle^b + \left(\frac{1}{\mathrm{Pe}} - \frac{1}{\exp(\mathrm{Pe}) - 1}\right)\langle c\rangle^d \tag{57}$$

where P_m is the effective membrane diffusivity permeability (i.e., the overall mass transfer coefficient with respect to the inner membrane surface area) and

$$\mathrm{Pe} = \frac{J_v}{P_m} \tag{58a}$$

is the Peclet number based on the ultrafiltration velocity. A comparison of Eqs. (55) and (56) reveals that this Peclet number corresponds to

$$\mathrm{Pe} = \frac{(a_b h_{tb} + a_d h_{td} + \omega)\omega}{a_d h_{td}(a_b h_{tb} + \omega)} \tag{58b}$$

which for the case of very thin membranes with $h_{tb} = h_{td}$ gives the following relation:

$$\frac{\omega}{a_b h_{td}} = \frac{\sqrt{4 + \mathrm{Pe}^2} + \mathrm{Pe} - 2}{2\mathrm{Pe}} \tag{59}$$

Thus, Eq. (54) may be written as

$$\langle c\rangle^m = \frac{\mathrm{Pe} - 2 + \sqrt{4 + \mathrm{Pe}^2}}{2\mathrm{Pe}}\langle c\rangle^b + \left(1 - \frac{\mathrm{Pe} - 2 + \sqrt{4 + \mathrm{Pe}^2}}{2\mathrm{Pe}}\right)\langle c\rangle^d \tag{60}$$

which naturally yields $\langle c\rangle^m = \left(\langle c\rangle^b + \langle c\rangle^d\right)/2$ for small ultrafiltration velocity (i.e., $\mathrm{Pe} \ll 1$) and $\langle c\rangle^m = \langle c\rangle^b$ for large ultrafiltration velocity (i.e., $\mathrm{Pe} \gg 1$). In Fig. 4, Eq. (60) based on the present model and the Kedem–Katchalsky model given by Eq. (57) is compared in terms of

$$\frac{\left(\langle c\rangle^m - \langle c\rangle^d\right)}{\left(\langle c\rangle^b - \langle c\rangle^d\right)}$$

which shows fairly a good agreement with each other.

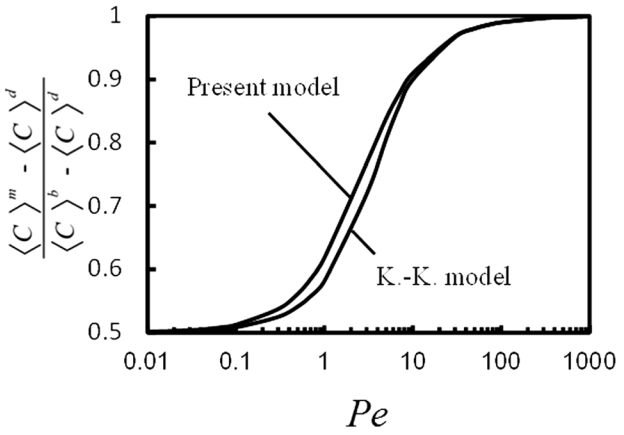

Fig. 4 Comparison of the present model and Kedem–Katchalsky model

Substitution of Eq. (54) into the solute transport equation (43) yields

$$\frac{d}{dx} u_b \langle c\rangle^b = -\frac{a_b h_{tb} a_d h_{td}}{a_b h_{tb} + a_d h_{td} + \omega}\left(\langle c\rangle^b - \langle c\rangle^d\right) - \omega\langle c\rangle^b \tag{61}$$

Furthermore, adding Eqs. (43) and (44), one has

$$u_b\langle c\rangle^b + u_d\langle c\rangle^d = u_b(1)\langle c\rangle^b(1) + u_d(1)\langle c\rangle^d(1) = (C_u - u_d(1))\langle c\rangle^b(1) = \text{const.} \tag{62}$$

where the solute concentration in the dialysate at the inlet $\langle c\rangle^d(1)$ is assumed to be zero. Upon noting $\langle c\rangle^b \frac{du_b}{dx} = -\omega\langle c\rangle^b$ the foregoing two equations can be combined to give

$$\frac{d}{dx}\langle c\rangle^b = -\left(\frac{a_b h_{tb} a_d h_{td}}{a_b h_{tb} + a_d h_{td} + \omega}\right)\frac{C_u\langle c\rangle^b - (C_u - u_d(1))\langle c\rangle^b(1)}{u_b(C_u - u_b)} \tag{63}$$

For the given solute concentration in the blood at the inlet $\langle c\rangle^b(0)$, this equation can be solved to give

$$\frac{\langle c\rangle^b(x^*)}{\langle c\rangle^b(0)} = \frac{1 - \frac{u_d(1)}{C_u}\left(1 - e^{f(1) - f(x^*)}\right)}{1 - \frac{u_d(1)}{C_u}\left(1 - e^{f(1)}\right)} \tag{64a}$$

Hence

$$\frac{\langle c\rangle^d(x^*)}{\langle c\rangle^b(0)} = \frac{u_b(1) - \left(1 - \frac{u_d(1)}{C_u}\left(1 - e^{f(1) - f(x^*)}\right)\right)u_b(x^*)}{\left(1 - \frac{u_d(1)}{C_u}\left(1 - e^{f(1)}\right)\right)(C_u - u_b(x^*))} \tag{64b}$$

where

$$f(x^*) = a_b h_{tb} a_d h_{td} L \int_0^{x^*} \frac{dx^*}{(a_b h_{tb} + a_d h_{td} + \omega(x^*)) u_b(x^*) \left(1 - \frac{u_b(x^*)}{C_u}\right)}$$
$$= \frac{1}{\mathrm{Pe}_m} \int_0^{x^*} \frac{dx^*}{\left(1 + \frac{\mathrm{Pe}_m}{2 + \frac{a_d h_{td}}{a_b h_{tb}} + \frac{a_b h_{tb}}{a_d h_{td}}} \left(\frac{\omega(x^*)L}{u_b(0)}\right)\right) \frac{u_b(x^*)}{u_b(0)} \left(1 - \frac{u_b(x^*)}{C_u}\right)} \cong \frac{1}{\mathrm{Pe}_m} \int_0^{x^*} \frac{dx^*}{\left(1 + \frac{\mathrm{Pe}_m}{4} \left(\frac{\omega(x^*)L}{u_b(0)}\right)\right) \frac{u_b(x^*)}{u_b(0)} \left(1 - \frac{u_b(x^*)}{C_u}\right)} \tag{65}$$

The dimensionless function $f(x^*)$ can be evaluated numerically using any standard integration scheme such as Runge–Kutta–Gill method (see e.g., Ref. [18]). The modified Peclet number, Pe_m, is defined as

$$\mathrm{Pe}_m = \left(\frac{1}{a_b h_{tb}} + \frac{1}{a_d h_{td}}\right) \frac{u_b(0)}{L} \cong \frac{d_b^2 u_b(0)}{8 \varepsilon_b \varepsilon_p D_m L} \ln\left(1 + 2\frac{t_m}{d_b}\right) \tag{66}$$

since

$$\frac{1}{a_b h_{tb}} + \frac{1}{a_d h_{td}} = \frac{1}{a_b h_b} + \frac{1}{a_d h_d} + \frac{d_b^2}{8 \varepsilon_b \varepsilon_p D_m} \ln\left(1 + 2\frac{t_m}{d_b}\right)$$
$$\cong \frac{d_b^2}{8 \varepsilon_b \varepsilon_p D_m} \ln\left(1 + 2\frac{t_m}{d_b}\right) \tag{67}$$

When the blood velocity is fixed, Pe_m may simply be regarded as a dimensionless total mass transfer resistance. The perfusion rate $\omega(x^*)$ and the blood Dacian velocity $u_b(x^*)$ are given by Eqs. (49) and (51), respectively. For the case of small metabolites clearances, one has $\omega(x^*) \ll a_b h_{tb} + a_d h_{td}$. Then, Eq. (65) simplifies to

$$f(x^*) = \frac{1}{\mathrm{Pe}_m} \int_0^{x^*} \frac{dx^*}{\frac{u_b(x^*)}{u_b(0)} \left(1 - \frac{u_b(x^*)}{C_u}\right)} \tag{68}$$

So far, five important dimensionless parameters are introduced. These are the inlet velocity ratio $u_d(1)/u_b(0)$, the permeability ratio α, the dimensionless membrane permeability α, the dimensionless transmembrane pressure β, and the modified Peclet number Pe_m. As these independent parameters are specified, the dimensionless solution concentrations can be determined uniquely using Eqs. (49), (51), (64*a*), (64*b*), and (68).

Clearance. The primary interest in this study, namely, the clearance of the solute from blood to dialysate CL is given by

$$\mathrm{CL} = A \frac{u_b(0)\langle c\rangle^b(0) - u_b(1)\langle c\rangle^b(1)}{\langle c\rangle^b(0)}$$
$$= A u_b(0) \left(1 - \frac{C_u - u_d(1)}{u_b(0)\left(1 - \frac{u_d(1)}{C_u}\left(1 - e^{f(1)}\right)\right)}\right) \tag{69}$$

The clearance CL is often used for the scale for the dialysis time. For the initial total body fluid volume V_b for recirculation, the dimensionless dialysis time may be defined as

$$t^* = \frac{\mathrm{CL}}{V_b} t \tag{70}$$

which is often designated as "KT/V" by dialyzer practitioners and is usually set to around 1.2 or more. The temporal description of the balance of total solute mass may be given by

$$\frac{d}{dt}(V_b - A(u_b(0) - u_b(1))t)\langle c\rangle^b = -\mathrm{CL}\langle c\rangle^b \tag{71}$$

Thus, after dialyzing for the time period $t^* = \mathrm{CL}t/V_b$, the solute concentration $\langle c\rangle^b(1;t^*)$ will be reduced to

$$\frac{\langle c\rangle^b(1;t^*)}{\langle c\rangle^b(0;0)} = (1 - \gamma t^*)^{\left(\frac{1}{\gamma} - 1\right)} \tag{72}$$

where

$$\gamma = \frac{A(u_b(0) - u_b(1))}{\mathrm{CL}} = \frac{1 - \frac{C_u - u_d(1)}{u_b(0)}}{1 - \frac{C_u - u_d(1)}{u_b(0)\left(1 - \frac{u_d(1)}{C_u}\left(1 - e^{f(1)}\right)\right)}} \tag{73}$$

For the case of removal of small metabolites such as urea, γ is small. Then, Eq. (72) reduces to the conventional formula which may be used for a rough estimation

$$\frac{\langle c\rangle^b(1;t^*)}{\langle c\rangle^b(0;0)} = e^{-t^*} \tag{74}$$

Closed Form Solutions for the Case of Pure Diffusion

There exist some special cases in which closed analytic solutions are possible. Such cases, namely, the case of no ultrafiltration (i.e., pure diffusive clearance) and the case of symmetry flow rates (i.e., $C_u = 0$), are investigated below. For this case of no ultrafiltration, one has $K_m = 0$, hence

$$B = 0 \tag{75a}$$

$$\beta = 0 \tag{75b}$$

$$u_b(x^*) = u_b(0) \tag{75c}$$

and

$$u_d(x^*) = u_d(1) \tag{75d}$$

$$f(x^*) = \frac{C_u x^*}{\mathrm{Pe}_m u_d(1)} = \frac{\left(\frac{1}{u_b(0)} + \frac{1}{u_d(1)}\right) L}{\left(\frac{1}{a_b h_{tb}} + \frac{1}{a_d h_{td}}\right)} x^* \tag{76}$$

Thus, the pure diffusive clearance CL_0 is given by

$$CL_0 = Au_b(0)\frac{\exp\left(\frac{1+\frac{u_b(0)}{u_d(1)}}{Pe_m}\right)-1}{\exp\left(\frac{1+\frac{u_b(0)}{u_d(1)}}{Pe_m}\right)+\frac{u_b(0)}{u_d(1)}} = Au_b(0)\frac{\exp\left(\frac{\frac{1}{u_b(0)}+\frac{1}{u_d(1)}}{\frac{1}{a_b h_{tb}}+\frac{1}{a_d h_{td}}}L\right)-1}{\exp\left(\frac{\frac{1}{u_b(0)}+\frac{1}{u_d(1)}}{\frac{1}{a_b h_{tb}}+\frac{1}{a_d h_{td}}}L\right)+\frac{u_b(0)}{u_d(1)}} \quad (77)$$

For the case of $Pe_m = 0.68$, and $\alpha = 2.53$, the velocity and solute concentration variations along the length of the dialyzer are indicated in Fig. 5, in which the two cases, namely, $u_d(1)/u_b(0) = -2$ and -3, are treated. Higher dialysate velocity $-u_d(1)/u_b(0)$ results in lowering solute concentrations at both exits.

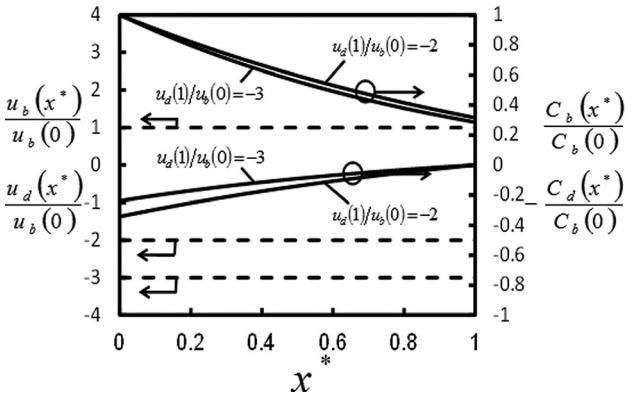

Fig. 5 Velocity and solute variations along the axial coordinate for the case of pure diffusion

Closed Form Solutions for the Case of Symmetric Flow Rates

For this case, the transmembrane pressure for given B associated with the membrane permeability is set as follows:

$$\beta = \frac{B}{\sinh B}\left(\cosh B + \frac{u_d(1)}{u_b(0)}\right) \quad (78)$$

such that Eq. (52) yields

$$u_b(x^*) + u_d(x^*) = C_u = 0 \quad (79)$$

For the case of removal of small metabolites, $\omega(x^*) \ll a_b h_{tb} + a_d h_{td}$ is satisfied. Hence

$$\frac{d}{dx}\langle c\rangle^b = \left(\frac{a_b h_{tb} a_d h_{td}}{a_b h_{tb} + a_d h_{td} + \omega}\right)\frac{u_d(1)\langle c\rangle^b(1)}{u_b^2} \cong \frac{1}{Pe_m}\left(\frac{u_b(0)u_d(1)\langle c\rangle^b(1)}{L}\right)\frac{1}{u_b^2} \quad (80)$$

where

$$u_b(x^*) = \frac{u_b(0)\sinh(B(1-x^*)) - u_d(1)\sinh Bx^*}{\sinh B} \quad (81)$$

Equation (80) with Eq. (81) may readily be integrated for given solute concentration in the blood at the inlet $\langle c\rangle^b(0)$

$$\frac{\langle c\rangle^b(x^*)}{\langle c\rangle^b(0)} = 1 + \frac{\frac{1}{Pe_m}\frac{u_d(1)}{u_b(0)}\frac{\sinh B}{B\left(e^{-B}+\frac{u_d(1)}{u_b(0)}\right)}\left(\frac{2\sinh B}{e^B+\frac{u_d(1)}{u_b(0)}-\left(e^{-B}+\frac{u_d(1)}{u_b(0)}\right)e^{2Bx^*}}-1\right)}{1-\frac{1}{Pe_m}\frac{u_d(1)}{u_b(0)}\frac{\sinh B}{B\left(e^{-B}+\frac{u_d(1)}{u_b(0)}\right)}\left(\frac{2\sinh B}{e^B+\frac{u_d(1)}{u_b(0)}-\left(e^{-B}+\frac{u_d(1)}{u_b(0)}\right)e^{2B}}-1\right)} \quad (82)$$

$$CL = Au_b(0)\left(1+\frac{\frac{u_d(1)}{u_b(0)}}{1-\frac{1}{Pe_m}\frac{u_d(1)}{u_b(0)}\frac{\sinh B}{B\left(e^{-B}+\frac{u_d(1)}{u_b(0)}\right)}\left(\frac{2\sinh B}{e^B+\frac{u_d(1)}{u_b(0)}-\left(e^{-B}+\frac{u_d(1)}{u_b(0)}\right)e^{2B}}-1\right)}\right) \quad (83)$$

Figure 6 shows the axial variations of the velocity and solute concentration fields for the cases of $B = 0.21$ (i.e., $\beta = 0.52$), $-u_d(1)/u_b(0) = 0.5$ and $\alpha = 2.53$, with $Pe_m = 0.68$ and 1.69. As can be seen from the figure, an increase in the modified Peclet number (i.e., dimensionless mass transfer resistance) retards reduction of the solute concentration in the blood at the exit.

Comparison of the Present Analytic Results and Available Experimental Data

For given dimensionless system parameters, namely, the lumen and shell permeability ratio α and the membrane permeability dimensionless parameter B, one only needs to specify the inlet velocity ratio $-u_d(1)/u_b(0)$, the modified Peclet number Pe_m

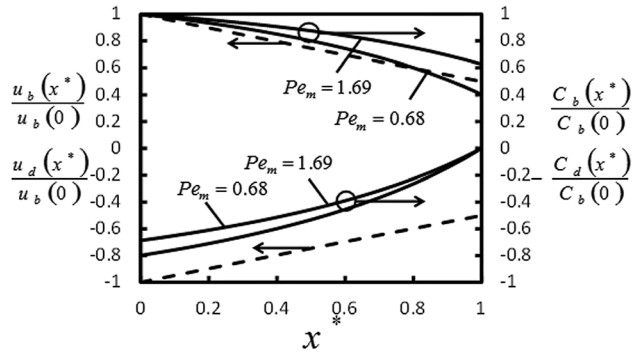

Fig. 6 Velocity and solute variations along the axial coordinate for the case of symmetric flow rates

(i.e., dimensionless mass transfer resistance), and the dimensionless transmembrane pressure at the blood inlet β. However, in many practical cases, the total ultrafiltration rate $A(u_b(0) - u_b(1))$ is provided instead of the transmembrane pressure. For such cases of the given total ultrafiltration rate, the transmembrane pressure at the blood inlet β may be evaluated using Eq. (52) as follows:

$$\beta = \frac{B}{\sinh B}\left(\cosh B + \frac{u_d(1)}{u_b(0)} - \frac{\alpha + \cosh B}{1+\alpha} \times \left(1 + \frac{u_d(1)}{u_b(0)} - \frac{(A(u_b(0) - u_b(1)))}{Au_b(0)}\right)\right) \tag{84}$$

Jaffrin et al. [26] carried out a series of experiments with a Hospal Filtral 12 AN69HF module using saline in substitution of the blood. Clearances for the two solutes, namely, creatinine (113 Da) and vitamin B12 (1355 Da) are predicted by the present model and are compared with their experimental data. Fortunately, detailed information is available for these two solutes. Geometric characteristics of the membrane module are provided by the manufacturer as follows:

$$L = 20 \text{ cm}, \quad N = 8500, \quad d_b = 220\ \mu\text{m}, \quad t_m = 45\ \mu\text{m}, \quad A = 11.94 \text{ cm}^2, \quad a_b = 4920/\text{m}$$

while the hydraulic permeability of the membrane L_p and the overall mass transfer coefficient P_m are provided by Ding et al. [12] as follows:

$$L_p = 5.63 \times 10^{-11}\text{m/sPa}, P_m(\text{creatinine}) = 4.172 \times 10^{-6}\text{m/s}, P_m(\text{vitaminB}_{12}) = 1.675 \times 10^{-6}\text{m/s}$$

The modified Peclet number Pe_m is evaluated using the overall mass transfer coefficient P_m as

$$\text{Pe}_m = \left(\frac{1}{a_b h_{tb}} + \frac{1}{a_d h_{td}}\right)\frac{u_b(0)}{L} = \frac{u_b(0)}{a_b L P_m} \tag{85}$$

Figure 7 shows the pure diffusive clearances CL_0 as a function of the inlet blood flow rate $Au_b(0)$ when the dialysate inlet volume flow rate is $Au_d(1) = -500$ ml/min. The figure shows a good agreement between the present analysis and the experiment reported by Jaffrin et al. [26]. For the case of $Au_b(0) = 200$ ml/min ($u_b(0) = 0.00279$ m/s) and $Au_d(1) = -500$ ml/min ($u_b(0) = 0.00698$ m/s)) , a series of clearances are calculated for the given total ultrafiltration rate $A(u_b(0) - u_b(1))$. This is done by assigning the dimensionless transmembrane pressure β according to Eq. (84). The errors in the clearance measurements are estimated to be less than 8 ml/min. In Fig. 8, the predicted $(\text{CL} - \text{CL}_0)/\text{CL}_0$ are plotted against the predicted ultrafiltration volume flow rate

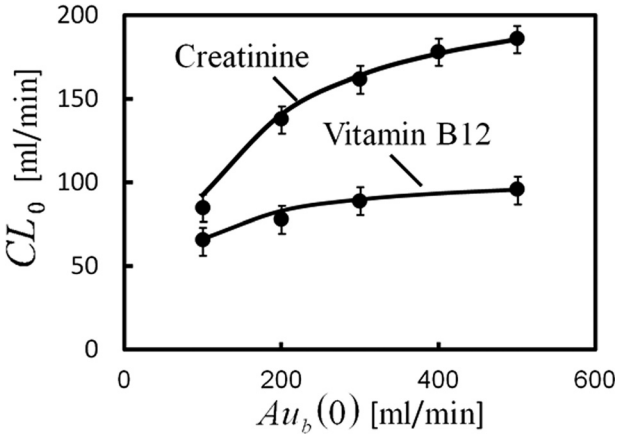

Fig. 7 Effect of blood flow velocity on the pure diffusive clearance of solutes (●:Experiment by Jaffrin et al. [25] ——, : Present model; $L = 20$ cm, $N = 8500$, $d_b = 220\ \mu$m, $t_m = 45\ \mu$m, $A = 11.94$ cm^2, $L_p = 5.63\times10^{-11}$m/sPa, P_m(creatinine) $= 4.172\times10^{-6}$m/s, P_m(vitaminB12) $= 1.675\times10^{-6}$m/s)

$A(u_b(0) - u_b(1))$ with the experimental data obtained by Jaffrin et al. Since the ultrafiltration rate is much less than the pure diffusion rate for the case of creatinine, the corresponding $(\text{CL} - \text{CL}_0)/\text{CL}_0$ is much small. Naturally, its difference between the prediction and experiment appears to be rather discernible. It is interesting to note that both analysis and experiment suggest that an almost linear relationship exists between $(\text{CL} - \text{CL}_0)/\text{CL}_0$ and $A(u_b(0) - u_b(1))$. In fact, the following approximate linear relationship may be derived after some manipulations using (64*a*), (69), and (77):

$$\frac{\text{CL} - \text{CL}_0}{\text{CL}_0} \cong \frac{\frac{1}{u_b(0)} + \frac{1}{u_d(1)}}{\exp\left(a_b P_m L\left(\frac{1}{u_b(0)} + \frac{1}{u_d(1)}\right)\right) - 1}(u_b(0) - u_b(1)) \tag{86}$$

The foregoing approximate relationship is presented by dashed lines in Fig. 8, which shows a good agreement with both the experiment and analysis especially for the case of vitamin B12. The errors between the full analysis and approximate relationship within the range studied here are estimated as 5% and 25% for

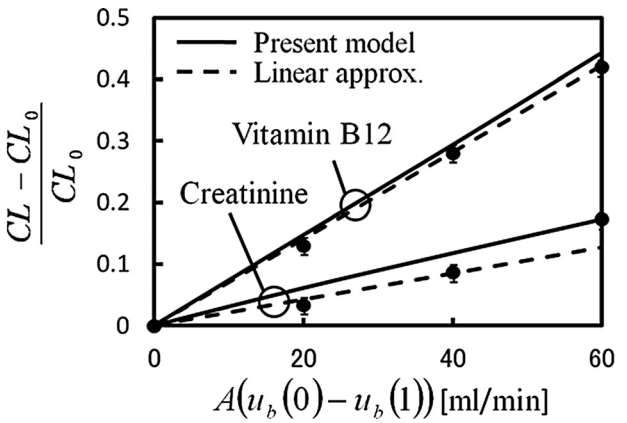

Fig. 8 Effect of ultrafiltration flow rate on the clearance enhancement (●:Experiment by Jaffrin et al. [26] ——, : Present model; ——— : Linear approximation; $L = 20$ cm, $N = 8500$, $d_b = 220\ \mu$m, $t_m = 45\ \mu$m, $A = 11.94$ cm^2, $L_p = 5.63\times10^{-11}$m/sPa, P_m(creatinine) $= 4.172\times10^{-6}$m/s, P_m(vitaminB12) $= 1.675\times10^{-6}$m/s, $Au_b(0) = 200$ml/min, $Au_d(1) = -500$ml/min)

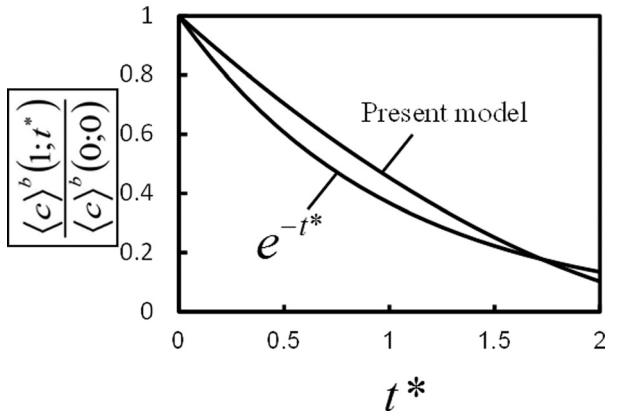

Fig. 9 Temporal variation of the solute concentration (creatinine: $A(u_b(0) - u_b(1)) = 60$ ml/min, $V_b = 42,000$ml, CL = 164.8 ml/min, $\gamma = 0.364$)

vitamin B12 and creatinine, respectively. This linear relationship between $(CL - CL_0)/CL_0$ and $A(u_b(0) - u_b(1))$ may be quite useful for practical estimations of the clearance for the given total ultrafiltration rate $A(u_b(0) - u_b(1))$. The use of this linear relationship, however, is limited to the case of moderate ultrafiltration rate, since the linearity ceases to be valid for large ultrafiltration rates.

Finally, the temporal variation of creatinine concentration in the same dialyzer is evaluated for the case of ultrafiltration volume flow rate $A(u_b(0) - u_b(1)) = 60$ ml/min and the initial total blood volume $V_b = 42,000$ml (N.B. CL = 164.8 ml/min and $\gamma = 0.364$) and is plotted in Fig. 9 along with the conventional exponential decay curve. It can be seen from the figure that the solute concentrations decrease rapidly for an initial recirculation period (say, $t^* = KT/V < 1$) and then diminish further gradually. The dynamic curve based on the present model reveals that the estimation based on the exponential decay curve may not be accurate especially for the case of removal of comparatively large metabolites. However, around the time range that the dialyzer practitioners set (say, $1.2 < t^* = KT/V < 2$), both results are fairly close. Thus, the use of the exponential decay curve in the therapy of hemodialysis may well be justified.

Conclusions

A rigorous mathematical development based on volume-averaging theory has been presented for obtaining a complete set of the volume-averaged governing equations for countercurrent fiber membrane dialyzer systems. Assigning three individual concentrations for the blood, dialysate, and membrane, the microscopic governing equations were averaged over a local control volume. Then, the resulting correlations associated with the spatial deviations were modeled, following the procedure previously established by Nakayama and Kuwahara for deriving a general bioheat equation. These macroscopic transient three-dimensional governing equations were reduced to the set of ordinary differential equations for the steady one-dimensional case. The set of the equations was solved to find Eqs. (64*a*) and (64*b*) which together with Eqs. (49), (51), and (65) provide the solution concentration distributions in both blood and dialysate. Such analytic expressions for the solution concentration distributions are not found elsewhere. Closed form solutions were obtained for the two special cases, namely, the case of pure diffusion and the case of symmetry flow rates. In order to verify the validity of the present three concentration model, numerical integrations were carried out using Runge–Kutta–Gill method, and the results were compared with available experimental data. A comparison between the analysis and experiment reveals that the present model is fully capable of describing complex transport process associated with countercurrent dialyzer systems. Furthermore, a linear relationship is found between the clearance increase and the ultrafiltration volume flow rate. A useful approximate equation is provided for practical estimations of the clearance for the given ultrafiltration volume flow rate. The present study is just a first step toward a complete three-dimensional numerical analysis based on the full set of the macroscopic governing equations derived here. Such a numerical study is underway.

Acknowledgment

The authors gratefully acknowledge invaluable technical supports provided by Mr. R. Imai, Department head of Clinical Engineering, Shizuoka Institute of Medical Care Science.

Nomenclature

A = cross-sectional area of the dialyzer case (m^2)
$Aint$ = interface between the fluid and membrane phases (m^2)
$a_{b,d}$ = specific surface area (1/m)
B = dimensionless parameter associated with membrane permeability
c = solute concentration (kg/m^3)
C_u = integration constant (m/s)
CL = clearance (m^3/s)
CL_0 = pure diffusive clearance (m^3/s)
$d_{b,d}$ = inner and outer diameters of the hollow fiber (m)
$D_{b,d,m}$ = solute diffusion coefficient (m^2/s)
D_{bdisjk} = dispersion tensor of the blood flow (m^2/s)
D_{ddisjk} = dispersion tensor of the dialysate flow (m^2/s)
d_p = diameter of cylindrical pore of the membrane (m)
$f(x^*)$ = dimensionless function
h = mass transfer coefficient (m/s)
h_t = effective mass transfer coefficient (m/s)
J_V = ultrafiltration velocity (m/s)
$K_{b,d,m}$ = permeability (m^2)
L = effective length of the dialyzer case (m)
L_p = hydraulic permeability of membrane (m/s Pa)
n_i = unit vector pointing outward from the fluid side to membrane side
p = pressure (Pa)
Pe = $Pe = J_V/P_m$: Peclet number
Pe_m = $Pe_m = u_b(0)/a_b L P_m$: modified Peclet number
P_m = effective membrane diffusivity permeability (overall mass transfer coefficient) (m/s)
r = radial coordinate (m)
t = time (s)
t_m = membrane thickness (m)
u_b = Dacian velocity of the blood (m/s)
u_d = Dacian velocity of the dialysate (m/s)
u_i = velocity vector (m/s)
V = representative elementary volume (m^3)
V_b = initial total volume of blood (m^3)
x = axial coordinate (m)
x^* = x/L = dimensionless axial coordinate

Greek Symbols

α = permeability ratio
β = dimensionless transmembrane pressure at the blood inlet
γ = $\gamma = A(u_b(0) - u_b(1))/CL$ = dimensionless parameter
$\varepsilon_{b,d,m}$ = volume fraction
ε_p = porosity of the membrane
μ = viscosity (Pa s)
Π = osmotic pressure (Pa)

ρ = density (kg/ m^3)
ω = perfusion rate (1/s)

Special Symbols

$\tilde{\phi}$ = deviation from intrinsic average
$\langle\phi\rangle$ = Darcian average
$\langle\phi\rangle^{b,d,m}$ = intrinsic average

Subscripts and Superscripts

b = blood
d = dialysate
m = membrane
dis = dispersion
f = fluid

References

[1] Kedem, O., and Katchalsky, A., 1958, "Thermodynamics Analysis of the Permeability of Biological Membranes to Non-Electrolytes," Biochim. Biophys. Acta, **27**, pp. 229–246.
[2] Lu, J.-F., and Lu, W.-Q., 2010, "A Numerical Simulation for Mass Transfer Through the Porous Membrane of Parallel Straight Channels," Int. J. Heat Mass Transfer, **53**, pp. 2404–2413.
[3] Tu, J.-W., Ho, C.-D., and Chuang, C.-J., 2009, "Effect of Ultrafiltration on the Mass-Transfer Efficiency Improvement in a Parallel-Plate Countercurrent Dialysis System," Desalination, **242**, pp. 70–83.
[4] Tu, J.-W., Ho, C.-D., and Yeh, H.-M., 2006, "The Analytical and Experimental Studies of the Parallel-Plate Concurrent Dialysis System Coupled With Ultrafiltration," J. Membr. Sci., **281**, pp. 676–684.
[5] Yeh, H. M., 2009, "Numerical Analysis of Mass Transfer in Double-Pass Parallel-Pale Dialyzers With External Recycle," Comput. Chem. Eng., **33**, pp. 815–821.
[6] Legallais, C., Catapano, G., Von Harten, B., and Baurmeister, U., 2000, "A Theoretical Model to Predict the Vitro Performance of Hemodiafilters," J. Membr. Sci., **168**, pp. 3–15.
[7] Palaty, Z., Zakova, A., and Petrik, P., 2006, "A Simple Treatment of Mass Transfer Data in Continuous Dialyzer," Chem. Eng. Proc., **45**, pp. 806–811.
[8] Galach, M., Ciechanowska, A., Sabalinska, S., Waniewski, J., Wojcicki, J., and Werynski, A., 2003, "Impact of Convective Transport on Dialyzer Clearance," J. Artif. Organs, **6**, pp. 42–48.
[9] Yeh, H. M., Cheng, T.-W., and Wu, H.-H., 1998, "Membrane Ultrafiltration in Hollow-Fiber Module With the Consideration of Pressure Declination Along the Fibers," Sep. Purif. Technol., **13**, pp. 171–180.
[10] Sigdell, J. E., 1982, "Calculation of Combined Diffusive and Convective Mass Transfer," Int.J. Artif. Organs, **5**(6), pp. 361–372.
[11] Waniewski, J., 2006, "Mathematical Modelling of Fluid and Solute Transport in Hemodialysis and Peritoneal Dialysis," J. Membr. Sci., **274**, pp. 24–37.
[12] Ding, W.-P., He, L.-Q., Zhao, G., Zhang, H.-F., Shu Z.-Q., and Gao, D.-Y., 2004, "Double Porous Media Model for Mass Transfer of Hemodialyzers," Int. J. Heat Mass Transfer, **47**, pp. 4849–4855.
[13] Shirazian, S., Moghadassi, A., and Moradi, S., 2009, "Numerical Simulation of Mass Transfer in Gas-Liquid Hollow Fiber Membrane Contactors for Laminar Flow Conditions," Simul. Modell. Pract. Theory, **17**, pp. 708–718.
[14] Wang, Y., Brannock, M., Cox, S., and Leslie, G., 2010, "CFD Simulations of Membrane Filtration Zone in a Submerged Hollow Fiber Membrane Bioreactor Using a Porous Media Approach," J. Membr. Sci., **363**, pp. 57–66.
[15] Kumar, V., and Upadhyay, S. N., 2000, "Computer Simulation of Membrane Processes: Ultrafiltration and Dialysis Units," Comput. Chem. Eng., **23**, pp. 1713–1724.
[16] Cheng, P., 1978, "Heat Transfer in Geothermal Systems," *Advances in Heat Transfer*, Vol. 14, Academic Press, New York, pp. 1–105.
[17] Quintard, M., and Whitaker, S., 1993, "One and Two Equation Models for Transient Diffusion Processes in Two-Phase Systems," Adv. Heat Transfer, **23**, pp. 369–465.
[18] Nakayama, A., 1995, *PC-Aided Numerical Heat Transfer and Convective Flow*, CRC Press, Boca Raton, FL.
[19] Vafai, K., and Tien, C. L., 1981, "Boundary and Inertia Effects on Flow and Heat Transfer in Porous Media," Int. J. Heat Mass Transfer, **24**, pp. 195–203.
[20] Nakayama, A., and Kuwahara, F., 2008, "A General Bioheat Transfer Model Based on the Theory of Porous Media," Int. J. Heat Mass Transfer, **51**, pp. 3190–3199.
[21] Nakayama, A., Kuwahara, F., and Kodama, Y., 2006, "An Equation for Thermal Dispersion Flux Transport and Its Mathematical Modelling for Heat and Fluid Flow in a Porous Medium," J. Fluid Mech., **563**, pp. 81–96.
[22] Kuwahara, F., Nakayama, A., and Koyama, H., 1996, "A Numerical Study of Thermal Dispersion in Porous Media," ASME J. Heat Transfer, **118**, pp. 756–761.
[23] Yang, C., and Nakayama, A., 2010, "A Synthesis of Tortuosity and Dispersion in Effective Thermal Conductivity," Int. J. Heat Mass Transfer, **53**(15–16), pp. 3222–3230.
[24] Kuznetsov, A. V., and Nield, D. A., 2009, "Forced Convection With Counterflow in a Circular Tube Occupied by a Porous Medium," J. Porous Media, **12**, pp. 657–666.
[25] Waniewski, J., Werynski, A., Ahrenholtz, P., Lucjanek, O., Judycki, W., and Esther, G., 1991, "Theoretical Basis and Experimental Verification of the Impact of Ultrafiltration on Dialyzer Clearance," Artif. Organs, **15**, pp. 70–77.
[26] Jaffrin, M. Y., Ding, L., and Laurent, J. M., 1990, "Simultaneous Convective and Diffusive Mass Transfer in a Hemodialyzer," J. Biomech. Eng., **112**, pp. 212–219.